
A Cross-Domain Benchmark for Active Learning

Anonymous Authors

Abstract

Active Learning (AL) deals with identifying the most informative samples for labeling to reduce data annotation costs for supervised learning tasks. AL research suffers from the fact that lifts from literature generalize poorly and that only a small number of repetitions of experiments are conducted. To overcome this obstacles, we propose *ALBench*, the first active learning benchmark which includes tasks in computer vision, natural language processing and tabular learning. Furthermore, by providing an efficient greedy oracle, *ALBench* can be evaluated with 50 runs for each experiment. We will show, that both the cross-domain character and the large amount of repetitions are crucial for sophisticated evaluation of AL research. Concretely, we will show that the superiority of specific methods varies over the different domains, making it important to evaluate Active Learning with a cross-domain benchmark. Additionally, we show, that having a large amount of runs is crucial. With only conducting five runs as often done in the literature, the superiority of specific methods can strongly vary with the specific runs. This effect goes so far, that it may even happen that dedicated methods like *margin-sampling* are not able to outperform the random baseline.

1 Introduction

Deep neural networks (NN) have produced state-of-the-art results on many important supervised learning tasks. Since Deep NNs usually require large amounts of labeled training data, Active Learning (AL) deals with selecting the most informative samples out of a large pool of unlabeled data, so that only these samples need to be labeled. It has been shown that a small labeled set of this nature can be used to train well-performing models. In the last decade, many different algorithms for AL have been proposed and almost every method has reported lifts over all its predecessors,¹ However, real insights into the current state of AL are hard to draw from these works, due to the following reasons: 1. These works do not use a standardized evaluation setting with fixed datasets and baseline approaches. 2. Due to computational constraints, a lot of works do only a small amount of experimental runs, hence it is questionable whether the superiority of a specific approach can be concluded from the conducted experiments. 3. The works are only evaluated in a specific domain, such as computer vision or language processing. However, AL is a general principle of supervised learning, and thus methods should be evaluated in multiple domains to assess their capabilities.

While multiple benchmark suites have been proposed to solve problem 1, to the best of our knowledge, all of them are either limited in the domains they consider or do not do enough runs for conclusive results. Hence, the current state of the art in Active Learning is still not well-understood and principled shortcomings of different algorithms and whether they are domain-independent, are currently not identified.

¹Out of all considered algorithms for this paper, only BALD [7] did not claim a new SOTA performance in their result section.

Here we step in with *ALBench*, an active learning benchmark which covers multiple application domains and reports a large amount of runs per experiment, so that the significance of performance differences can be estimated. Specifically, *ALBench* consists of datasets from computer vision, natural language processing and the tabular domain. We provide our datasets both in raw format as well as “embedded” by a fixed embedding model, enabling evaluation of AL methods in this semi-supervised setting. Furthermore, we propose two novel synthetic datasets to highlight general challenges for AL methods.

The applied evaluation protocol in *ALBench* uses 50 runs for each experiment. By having such a large amount of runs, we can evaluate the significance of performance gaps and identify the best performing approaches for each dataset as well as whole domains. Furthermore, we show that the small amount of runs other works do in fact produce to misleading results. To be more specific, we show that if only 3 restarts are employed for each experiment, the performance of specific methods strongly varies. As we will see, even the ranking of the different methods averaged over many datasets fluctuates with the specific set of runs. This effect is so strong, that even for a well-established method such as margin-sampling, it’s performance can be significantly better and significantly worse than random for the same dataset, depending on the seed.

To enable the computation of an oracle performance for a protocol with large amounts of restarts we propose a *greedy oracle function* which uses only a small amount of search steps to estimate the optimal solution. While being more time-efficient than established oracle functions, it possibly underestimates the real upper bound performance. However, as our experiments will show, it is still outperforming all current AL methods by at least 5% and thus is suitable as an upper bound.

Our experimental evaluation shows, that there exists no clear SOTA method for Active Learning. The superiority of methods is strongly dataset- and domain-dependent with the outstanding observation, that the image domain works fundamentally different than the tabular and text domain. Here, the best performing approach for text and tabular data, namely *margin sampling*, is significantly outperformed by *least confident sampling*, which does not belong to the top performing approaches in any other domain. Thus, using the performance of Active Learning approaches on the image domain as a proxy of Active Learning in general, as it is often done [2, 19, 15, 10, 17], is questionable. To further analyze performance of common methods, we propose *Honeypot* and *Diverging Sin*, two synthetic datasets, designed to be challenging for naive decision-boundary- and clustering-based approaches respectively. Hence, they provide insights in principled shortcomings of AL methods.

To sum up, *ALBench* is an experimental framework which includes an efficient oracle approximation, multiple application domains, enough repetitions to draw valid conclusions and two synthetic tasks to highlight shortcomings of AL methods. By being the first benchmark to proving these things in one code-base, we believe that *ALBench* is a major step forward of assessing the overall state of Active Learning research, independent of specific application domains. *ALBench* is publicly available under *anonymous*.

Our contributions include the following:

1. We show that the small of repetitions that previous works have employed is not sufficient for meaningful conclusions. Sometimes even making it impossible to assess if a performance is above or below random.
2. We propose an efficient and performant oracle which is constructed iteratively in a greedy fashion, overcoming major computational hurdles.
3. We propose *IMTSBench*, the first general benchmark providing tasks in the domains of images, text and tabular learning. It further contains synthetic and pre-encoded data to allow for a sophisticated evaluation of AL methods. Our experiments show, that there is no clear state-of-the art method for active learning across different domains.
4. We propose *Honeypot* and *Diverging Sin*, two synthetic datasets designed to hinder active learning by naive decision-boundary- or clustering-based approaches respectively. Thus, they provide an important tool to identify shortcomings of existing AL methods.

Table 1: Comparison of our benchmark with the existing literature. Oracle curves serve as an approximation of the best possible AL algorithm. Including the encoded versions of our datasets we reach 14 datasets, without we have 9. "Semi" indicates whether the paper is employing any form of self- or semi-supervised learning. A "-" for repetitions means that we could not determine how often each experiment is repeated in the respective framework. *ALBench* is the only benchmark which reports over enough runs for meaningful results and considers all 5 domains.

Paper	Sampling	#Data	#Alg	Img	Txt	Tab	Synth	Semi	Oracle	Repetitions
Beck et al. [2]	batch	4	7	✓	-	-	-	-	-	-
Hu et al. [9]	batch	5	13	✓	✓	-	-	-	-	3
Zhou et al. [29]	batch	3	2	✓	✓	-	-	-	✓	5
Zhan et al. [27]	sngl+batch	35	18	-	-	✓	✓	-	✓	10-100
Munjal et al. [19]	batch	2	8	✓	-	-	-	-	-	3
Li et al. [15]	batch	5	13	✓	-	-	-	✓	-	-
Rauch et al. [22]	batch	11	5	-	✓	-	-	-	-	5
Ji et al. [10]	batch	3	8	✓	-	-	-	-	-	-
Lueth et al. [17]	batch	4	5	✓	-	-	-	✓	-	3
Ours	sngl+batch	9(14)	11	✓	✓	✓	✓	✓	✓	50

2 Problem Description

Given two spaces \mathcal{X}, \mathcal{Y} , $n = l + u$ data points with $l \in \mathbb{N}$ labeled examples $\mathcal{L} = \{(x_1, y_1), \dots, (x_l, y_l)\}$, $u \in \mathbb{N}$ unlabeled examples $\mathcal{U} = \{x_{l+1}, \dots, x_n\}$, a model $\hat{y} : \mathcal{X} \rightarrow \mathcal{Y}$, a budget $\mathbb{N} \ni b \leq u$ and an annotator $A : \mathcal{X} \rightarrow \mathcal{Y}$ that can label x . We call $x \in \mathcal{X}$, $y \in \mathcal{Y}$ predictors and labels respectively where (x, y) are drawn from an unknown distribution ρ . Find an acquisition function $\Omega : \mathcal{U}^{(i)}, \mathcal{L}^{(i)} \mapsto x^{(i)} \in \mathcal{U}^{(i)}$ that iteratively selects the next unlabeled point $x^{(i)}$ for labeling

$$\begin{aligned}\mathcal{L}^{(i+1)} &\leftarrow \mathcal{L}^{(i)} \cup \{(x^{(i)}, A(x^{(i)}))\} \\ \mathcal{U}^{(i+1)} &\leftarrow \mathcal{U}^{(i)} \setminus \{x^{(i)}\}\end{aligned}$$

with $\mathcal{U}^{(0)} = \text{seed}(\mathcal{U}, s)$ and $\mathcal{L}^{(0)} = (\mathcal{U}_i^{(0)}, A(\mathcal{U}_i^{(0)}))$ $i \in [1, \dots, s]$, where $\text{seed}(\mathcal{U}, s)$ selects s points per class for the initial labeled set.

So that the average expected loss $\ell : \mathcal{Y} \times \mathcal{Y} \rightarrow \mathbb{R}$ of a machine learning algorithm fitting $\hat{y}^{(i)}$ on the respective labeled set $\mathcal{L}^{(i)}$ is minimal:

$$\min \frac{1}{B} \sum_{i=0}^B \mathbb{E}_{(x,y) \sim \rho} \ell(y, \hat{y}^{(i)})$$

3 Related Work

While multiple benchmark suites have been proposed for Active Learning, none of them provide experiments for more than two domains. The authors of [2], [19], [15], [10] and [17] even focus exclusively on the image domain. Especially the tabular domain is underrepresented in preceding benchmarks, as only [28] provides experiments for it. Experiments on the interplay between AL and semi-supervised learning are similarly under-researched, as only two works exist [15, 17], both of them only using images. An oracle algorithm has been proposed by two works [29, 28]. Both of these algorithms rely on search and are computationally very expensive, while our proposed method efficiently can be constructed sequentially. The two closest related works to this benchmark are [10] and [17], who also place a much higher emphasis on the problem of evaluating AL algorithms under many forms of variance than their predecessors (indicated in Tab. 1 by a dashed line). The authors of [10] posed a total of 12 "recommendations" for reliable evaluation of AL algorithms. We largely adapt the proposed recommendations of [10] and extend their work to multiple domains, batch sizes and comparisons. For a complete list of the recommendations and our implementation of them, please refer to App. A. This work also pays attention to the so-called "pitfalls" of AL evaluation proposed in [17]. For a complete list of the pitfalls and our implementation of them, please refer to

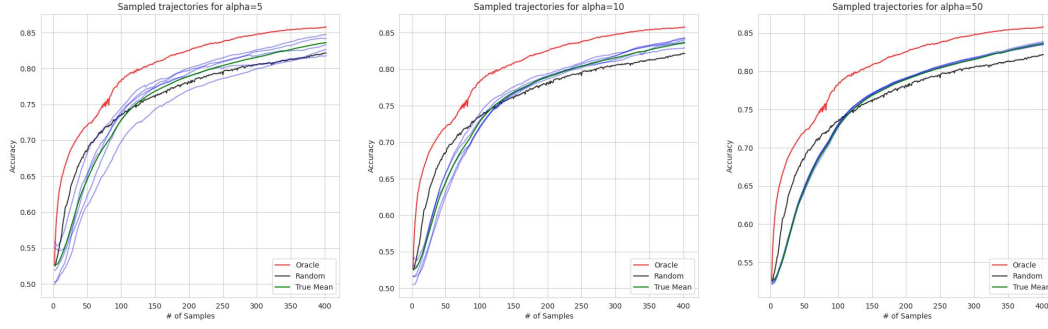


Figure 1: Random draws from a pool of 100 runs for margin sampling on the Splice dataset with different numbers of repetitions ($\alpha = \{5, 10, 50\}$). Green curves are the mean performance of all 100 runs, while the samples are blue. Even with 5 or 10 repetitions, we can observe that single draws for margin sampling display below-random performance (black), while the true mean should be above random.

109 App. B. To the best of our knowledge, we are the first to extend reliable SOTA (based on [10, 17])
 110 experimentation to a total of 5 data domains and a high number of restarts per experiment.

111 4 Few Repetitions are not Sufficient for Meaningful Results

112 To evaluate how many restarts are necessary to obtain conclusive results in an AL experiment, we
 113 computed 100 runs of our top-performing algorithm on one dataset. Our best algorithm is margin
 114 sampling and we chose the Splice dataset for its average size and complexity.
 115 This allows us firstly, to obtain a very strong estimation of the "true" average performance of margin
 116 sampling on this dataset and secondly, to draw subsets from this pool of 100 runs. Setting the size
 117 of our draws to α and sampling uniformly, we can approximate a cross-validation process with α
 118 restarts. Each of these draws can be interpreted as a **reported result in AL literature** where the
 119 authors employed α restarts. Figure 1 shows the "true" mean performance of margin sampling
 120 (green) in relation to random sampling (black) and the oracle performance (red). We display 5
 121 random draws of size α in blue. We can observe that even for a relatively high number of restarts the
 122 variance between the samples is extremely high, resulting in some performance curves being worse
 123 than random and some being significantly better. When setting $\alpha = 50$ we observe all samples to
 124 converge close to the true mean performance. In addition to this motivating example, we carried
 125 out our main evaluation (Tab. 3) multiple times by uniformly sampling 3 random from our available
 126 runs and comparing the results. We found significant differences in the performance of acquisition
 127 functions on individual datasets, as well as permutations in the final ranking. This partly explains
 128 the ongoing difficulties in reproducing results for AL experiments and benchmarks. The details can
 129 be found in App. D. For this benchmark we employ 50 restarts of every experiment.

130 4.1 Seeding vs. Restarts

131 Considering the high computational cost of 50 repetitions, another approach to ensure consistency
 132 between experiments would be to reduce the amount of variance in the experiment by keeping as
 133 many subsystems (weight initialization, data splits, etc.) as possible fixed with specialized seeding.
 134 We describe a novel seeding strategy in Appendix H that creates 3 separate Random Number Gen-
 135 erators (RNG) based on 3 different seeds. In short, we introduce three different seeds: s_Ω for the
 136 AL algorithm, $s_\mathcal{D}$ for dataset splitting and mini-batch sampling, and s_θ for model initialization and
 137 sampling of dropout masks. Unless stated otherwise, we will keep s_Ω fixed, while $s_\mathcal{D}$ and s_θ are
 138 incremented by 1 between restarts to introduce stochasticity into our framework. While this seeding
 139 strategy is capable of controlling the amount variance in the experiment, previous works have noted

that an actively sampled, labeled set does not generalize well between model architectures or even different initializations of the same model ([29, 16]), providing a bad approximation of the quality of an AL algorithm (i.e. measured performances for an algorithm might not even transfer to a different model initialization). Hence, we opt for letting the subsystems vary (by increasing $s_{\mathcal{D}}$ and s_{θ}) and combine that with a high number of restarts to obtain a good average of the generalization performance of each AL algorithm. Where a high number of restarts is computationally not feasible, we advise to additionally keep either $s_{\mathcal{D}}$ or s_{θ} (or both) fixed.

5 ALBench: A Cross-Domain Active Learning Benchmark

A detailed description of the preprocessing of each dataset can be found in Appendix K.

Tabular: AL research conducted on tabular data is sparse (only [1] from the considered baseline papers). We, therefore, introduce a set of tabular datasets that we selected according to the following criteria: (i) They should be solvable by medium-sized models in under 1000 samples, (ii) the gap between most AL algorithms and random sampling should be significant (potential for AL is present) and (iii) the gap between the AL algorithms and our oracle should also be significant (research on these datasets can produce further lifts). We use **Splice**, **DNA** and **USPS** from LibSVMTools [20]. **Image:** We use **FashionMNIST** [25] and **Cifar10** [13], since both are widely used in AL literature. **Text:** We use **News Category** [18] and **TopV2** [6]. Text datasets have seen less attention in AL research, but most of the papers that evaluate on text ([9], [29]) use at least one of these datasets.

We would like to point out that these datasets are selected for speed of computation (both in terms of the required classifier and the necessary budget to solve the dataset). However, similar to our argumentation for picking smaller classifiers, we are solely focused on comparing different AL algorithms in this paper and do not aim to develop novel classification models on these datasets. Our assumption is that a well-performing algorithm in our benchmark will also generalize well to larger real-world datasets, because we included multiple different data domains and classifier sizes in our experiments.

Adapting the semi-supervised setting from [8], we offer all our datasets un-encoded (normal) as well as pre-encoded by a fixed embedding model that was trained by unsupervised contrastive learning. The text datasets are an exception to this, as they are only offered in their encoded form. Pre-encoded datasets enable us to test small query sizes on more complex datasets like **Cifar10** and **FashionMnist**. They also serve the purpose of investigating the interplay between self-supervised learning techniques and AL, as well as alleviating the cold-start problem described in [17] as they require a way smaller seed set. The classification model for every encoded dataset is a single linear layer with softmax activation. The embedding model was trained with the SimCLR [5] algorithm adopting the protocol from [8]. To ensure that enough information from the data is encoded by our embedding model, the quality of embeddings during pretext training was measured after each epoch. To this end, we attached a linear classification head to the encoder, fine-tuned it to the data and evaluated this classifier for test accuracy. The checkpoint of each encoder model will be provided together with the framework.

Every dataset has a fixed size for the seed set of 1 sample per class, with the only exceptions being un-encoded **FashionMnist** and **Cifar10** with 100 examples per class to alleviate the cold-start problem in these complex domains.

5.1 Batch Sizes

We selected batch sizes for each dataset to accommodate the widest range possible that results in a reasonable runtime for low batch sizes and allows for at least 4 round of data acquisition for high batch sizes. The available batch sizes per dataset can be found in Table 2.

5.2 Realism vs. Variance

Table 2: Employed model, chosen budget and available batch sizes for each dataset

	Model	B	1	5	20	50	100	500	1K
Enc. DNA	Linear	40	o	o					
Enc. Splice	Linear	100	o	o	o	o			
TopV2	BiLSTM	200	o	o	o	o			
Splice	MLP	400	o	o	o	o	o		
DNA	MLP	300	o	o	o	o	o		
USPS	MLP	400	o	o	o	o	o		
Enc. Cifar10	Linear	450	o	o	o	o	o		
Enc. FMnist	Linear	500	o	o	o	o	o		
Enc. USPS	Linear	600	o	o	o	o	o		
News	BiLSTM	3K			o	o	o	o	
FMnist	ResNet18	10K						o	o
Cifar10	ResNet18	10K						o	o

We would like to point out that some design choices for this framework prohibit direct transfer of our results to practical applications. This is a conscious choice, as we think that this is a necessary trade-off between realism and experiment variance. We would like to highlight the following design decisions:

- (i) Creating test and validation splits from the full dataset rather than only the labeled seed set. Fully fledged test and validation splits are unobtainable in practice, but they not only provide a better approximation of the algorithms generalization performance, but also a better foundation for hyperparameter tuning, which is bound to reduce variance in the experiment.
- (ii) Choosing smaller classifiers instead of SOTA models. Since we are not interested in archiving a new SOTA in any classification problem, we instead opt to use smaller classifiers for the following reasons: Smaller classifiers generally exhibit more stable training behavior, on average require fewer sampled datapoints to reach their full-dataset-performance and have faster training times. For every dataset, the chosen architecture’s hyperparameters are optimized to archive maximum full-dataset performance. Generally, we use MLPs for tabular, ResNet18 for image and BiLSTMs for text datasets. Every encoded dataset is classified by a single linear layer with softmax activation. The used model for each dataset can be found in Tab. 2. For a detailed description and employed hyperparameters please refer to Appendix K.

5.3 Evaluation Protocol

Following [29], the quality of an AL algorithm is evaluated by an “anytime protocol” that incorporates classification performance at every iteration, as opposed to evaluating final performance after the budget is exhausted. We employ the normalized area under the accuracy curve (AUC):

$$\text{AUC}(\mathcal{D}_{\text{test}}, \hat{y}, B) := \frac{1}{B} \sum_{i=1}^B \text{Acc}(\mathcal{D}_{\text{test}}, \hat{y}^{(i)}) \quad (1)$$

The AUC incorporates performance in early stages (low budget) as well as capabilities to push the classifier in later stages (high budget). AL algorithms have to perform well in both scenarios.

Since AUC is still influenced by the budget, we define a set of rules to set this hyperparameter upfront, so that we are not favoring a subset of algorithms by handcrafting a budget. In this work, we choose the budget per dataset to be the first point at which one of 2 stopping conditions apply: (i) an algorithm (except Oracle) manages to reach 99% of the full-dataset-performance (using the smallest query size) or (ii) the best algorithm (except oracle) did not improve the classifier’s accuracy by at least 2% in the last 20% of iterations. The first rule follows [10], while the second rule prevents excessive budgets for cases with diminishing returns in the budget. The resulting budgets can be found in Tab. 2.

As described in Sec. 4, we restart each experiment multiple times. Each restart retains the train/test split (often given by the dataset itself), but creates a new validation split that is sampled (based on $s_{\mathcal{D}}$) from the entire dataset (not just the seed set $\mathcal{L}^{(0)}$).

Apart from plotting standard performance curves and reporting their AUC values per dataset in App. G, we primarily rely on ranks to aggregate the performance of an acquisition function across datasets. For each dataset and query size, the AUC values of all acquisition functions are sorted and assigned a rank based on position, with the best rank being 1. These ranks can safely be averages across datasets as they are no longer subjected to scaling differences of each dataset. Additionally, we employ Critical Difference (CD) diagrams (like Fig. 2) for statistical testing. CD diagrams use the Wilcoxon signed-rank test, which is a variant of the paired T-test, to find significant differences of ranks between acquisition functions. For these diagrams, each combination of dataset, query

size and run is considered a separate experiment, i.e. the results of Dataset1-QuerySize1-run5 of an acquisition function x is only compared to the results of Dataset1-QuerySize1-run5 of acquisition function y . Due to the large number of restarts and the wide range of datasets and query sizes, we can provide very accurate significance tests. For a detailed description of how every CD diagram is created, please refer to App. F.

6 A Greedy Oracle Algorithm

A oracle method for AL tries to find the oracle set \mathcal{O}_b for a given dataset, model, and training procedure that induces the highest AUC score for a given budget. However, since this combinatorial problem is computationally infeasible for realistic datasets, previous works have proposed approximations to this oracle sequence. [29] used simulated annealing to search for the optimal subset and used the best solution found after a fixed time budget. Even though their reported performance curves display a significant lift over all other acquisition functions, we found the computational cost of reproducing this oracle for all our datasets to be prohibitive (The authors reported the search to take several days per dataset on 8 V100 GPUs). In this paper, we propose a greedy oracle algorithm that constructs an approximation of the optimal set in an iterative fashion. Our oracle algorithm evaluates every data point $u_k = \text{unif}(\mathcal{U}) \quad k \in [1 \dots \tau]$ in a subsample of unlabeled points by recovering the label, fitting the classifier \hat{y} on $\mathcal{L}^{(i)} \cup \{u_k\}$ and directly measuring the resulting test performance. The data point that incurs the largest lift in test performance is selected and added to the labeled pool for that iteration. Due to the algorithms greedy nature (just considering the next point to pick), our oracle frequently encounters situations where every point in u_k would incur a negative lift (worsening the test performance). This can happen, for example, if the oracle picked a labeled set that enables the classifier to correctly classify a big portion of easy samples in the test set, but now fails to find the next **single** unlabeled point that would enable the classifier to succeed on one of the hard samples. This leads to a situation, where no point can immediately incur an increase in test performance and therefore the selected data point can be considered random. To circumvent this problem, we use our best-performing acquisition function (margin sampling [24]) as a fallback option for the oracle. Whenever the oracle does not find an unlabeled point that results in an increase in performance, it defaults to margin sampling in that iteration. The resulting greedy algorithm constructs an approximation of the optimal labeled set that consistently outperforms all other algorithms by a significant margin, while requiring relatively low computational cost ($\mathcal{O}(B\tau)$). We fix $\tau = 20$ in this work, as this gave us an average lift of 5% over the best performing acquisition function per dataset (which is significant for AL settings) and we expect diminishing returns for larger τ . The pseudocode for our oracle can be found in App. L. Even though our proposed algorithm is more efficient than other approaches, the computational costs for high budget datasets like Cifar10 and FashionMnist meant that we could not compute the oracle for all 10000 datapoints. To still provide an oracle for these two datasets, we select two points per iteration instead of one and stop the oracle computation at a budget of 2000. The rest of the curve is forecast with a simple linear regression that asymptotically approaches the upper bound performance of the dataset. A detailed description can be found in App. I.

[Thorben]
Ich habe die Erklärung für den Fallback im Oracle neu gemacht. Ist das verständlich?

Da wir den Fallback haben, sollten wir das Oracle vielleicht einfach als Erweiterung von Margin-Sampling verkaufen?

7 Experiments

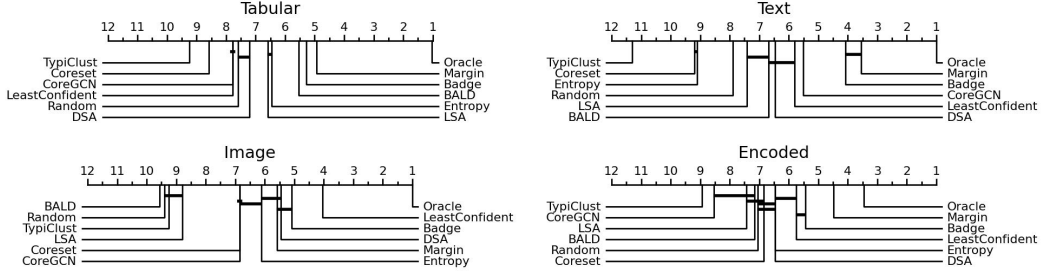
7.1 Implementation Details

At each iteration i the acquisition function Ω picks an unlabeled datapoint based on a fixed set of information $\{\mathcal{L}^{(i)}, \mathcal{U}^{(i)}, B, |\mathcal{L}^{(i)}| - |\mathcal{L}^{(1)}|, \text{acc}^{(i)}, \text{acc}^{(1)}, \hat{y}^{(i)}, \text{opt}_{\hat{y}}\}$, where $\text{opt}_{\hat{y}}$ is the optimizer used to fit $\hat{y}^{(i)}$. This set grants full access to the labeled and unlabeled set, as well as all parameters of the classifier and the optimizer. Additionally, we provide meta-information, like the size of the seed set through $|\mathcal{L}^{(i)}| - |\mathcal{L}^{(1)}|$, the remaining budget though the addition of B and the classifiers potential though $\text{acc}^{(1)}$ and $\text{acc}^{(i)}$. We allow acquisition functions to derive information from this set, e.g. predictions of the classifier $\hat{y}^{(i)}(x); \quad x \in \mathcal{U}^{(i)} \cup \mathcal{L}^{(i)}$, clustering, or even training additional models.

Table 3: Performances for acquisition functions on real-world datasets, aggregated for un-encoded and encoded datasets. Performance is shown as average ranks over restarts (1.0 is the best rank). Algorithms are sorted by aggregated performance on un-encoded datasets.

	Splice	DNA	USPS	Cifar10	FMnist	TopV2	News	Un-enc.	Enc.
Oracle	1.0 \pm 0.01	1.0 \pm 0.01	1.0 \pm 0.0	1.0 \pm 0.0	1.0 \pm 0.0	1.0 \pm 0.01	1.0 \pm 0.0	1.0	2.0
Margin	6.6 \pm 0.02	4.3 \pm 0.01	2.1 \pm 0.01	6.3 \pm 0.01	4.4 \pm 0.0	2.4 \pm 0.01	3.7 \pm 0.0	4.3	4.2
Badge	5.2 \pm 0.01	6.3 \pm 0.01	2.9 \pm 0.01	5.2 \pm 0.01	4.7 \pm 0.0	3.3 \pm 0.01	3.5 \pm 0.0	4.5	5.4
LeastConf	9.2 \pm 0.02	10.3 \pm 0.02	8.1 \pm 0.02	2.1 \pm 0.01	4.0 \pm 0.0	7.9 \pm 0.02	3.0 \pm 0.01	6.4	6.5
DSA	7.4 \pm 0.02	7.3 \pm 0.01	7.5 \pm 0.01	5.4 \pm 0.01	5.1 \pm 0.0	6.0 \pm 0.02	7.3 \pm 0.01	6.6	6.7
BALD	4.0 \pm 0.01	4.7 \pm 0.01	5.4 \pm 0.01	12.0 \pm 0.01	7.6 \pm 0.0	7.6 \pm 0.02	5.0 \pm 0.0	6.6	7.6
CoreGCN	6.9 \pm 0.01	4.9 \pm 0.01	10.4 \pm 0.01	7.6 \pm 0.01	6.5 \pm 0.01	4.0 \pm 0.01	6.8 \pm 0.0	6.7	8.2
Entropy	6.6 \pm 0.02	3.9 \pm 0.01	7.6 \pm 0.01	7.6 \pm 0.01	4.9 \pm 0.01	9.8 \pm 0.02	9.6 \pm 0.0	7.1	6.5
LSA	6.1 \pm 0.01	6.8 \pm 0.01	5.3 \pm 0.01	7.7 \pm 0.01	10.6 \pm 0.01	7.5 \pm 0.01	7.3 \pm 0.01	7.3	7.5
Random	9.0 \pm 0.01	9.3 \pm 0.01	5.3 \pm 0.01	8.4 \pm 0.01	11.1 \pm 0.0	7.9 \pm 0.01	8.0 \pm 0.0	8.4	6.9
Coreset	7.1 \pm 0.01	9.0 \pm 0.01	10.5 \pm 0.01	6.8 \pm 0.01	7.1 \pm 0.0	8.5 \pm 0.02	10.8 \pm 0.01	8.5	7.2
TypiClust	8.8 \pm 0.01	10.2 \pm 0.01	12.0 \pm 0.02	7.9 \pm 0.01	11.0 \pm 0.01	12.0 \pm 0.02	12.0 \pm 0.01	10.5	9.2

Figure 2: Ranks of each acquisition function aggregated by domain. Horizontal bars indicate a **non**-significant rank difference. The significance is tested via a paired-t-test with $\alpha = 0.05$.



However, the algorithm may not incorporate external information e.g. other datasets, queries to recover additional labels, additional training steps for \hat{y} , or the test/validation set.

For our study we selected acquisition functions with good performances reported by multiple different sources that can work with the set of information stated above. For a list of all acquisition functions, please refer to Table 3, with detailed descriptions being found in Appendix C.

The model \hat{y} can be trained in two ways. Either the parameters of the model are reset to a fixed initial setting $\hat{y}^{(0)}$ after each AL iteration and the classifier is trained from scratch with the updated labeled set $\mathcal{L}^{(i)}$, or the previous state $\hat{y}^{(i-1)}$ is retained and the classifier is fine-tuned on $\mathcal{L}^{(i)}$ for a reduced number of epochs. In this work, we use the fine-tuning method for un-encoded datasets to save computational time, while we use the from-scratch training for embedded datasets since they have very small classifiers and this approach generally produces better results. Our fine-tuning scheme always trains for at least one epoch and employs an aggressive early stopping with a patience of 2 afterwards.

7.2 Results on Real-world Data

In Table 3 we provide the rank of each acquisition function per dataset and averaged for each (un-)encoded dataset. Please note, that for Tab 3 we are averaging not only over runs, but also over query sizes per dataset. For the results per query size, please refer to App. E.

As stated in contribution C4, our results on real-world data shows significant differences in the performance of the tested algorithms between data domains. Not only do some algorithms overperform on some domains (like least confidence sampling on Images), but the Top-3 of algorithms (except Oracle) does not contain the same three algorithms for any two domains. Most interestingly, the image domain, which received the most attention in benchmarking so far could even be considered an outlier, as this is the only domain where the Top-1 algorithm changes. This highlights the dire need for diverse data domains in AL benchmarking.

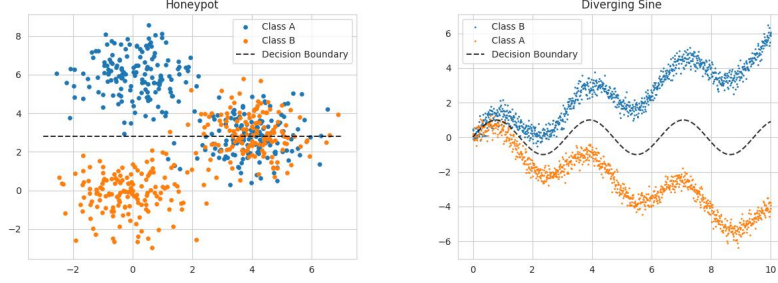


Figure 3: Synthetic "Honeyplot" and "Diverging Sine" datasets. The optimal decision boundary is not part of the dataset and serves only as a visual guide.

8 Honeyplot and Diverging Sine

AL approaches can be categorized into two types, uncertainty and geometric approaches. Typical members of the first category are variants of uncertainty sampling like entropy-, margin and least-confident-sampling [24] as well as BALD [7]. Typical members of the second category are clustering approaches like Coreset [23], BADGE [1] and TypiClust [8]. Both types of algorithms have principled shortcomings in terms of the utilized information that makes them unsuitable for certain data distributions. To test for these specific shortcomings, we created two synthetic datasets, namely "Honeyplot" and "Diverging Sine", that are hard to solve for methods focused on the classifier's decision boundary or data clustering respectively. To avoid algorithms memorizing these datasets they are generated from scratch for each experiment, depending on s_D .

Honeyplot creates two easy to distinguish clusters with 150 samples each and one overlapping "honeyplot" that represents a noisy region of the dataset with potentially miss-labeled, miss-measured or generally adverse samples. This honeyplot contains 150 samples of each class, creating a balance of 50% beneficial samples and 50% adverse samples in the dataset. The honeyplot is located on the likely decision boundary of a classifier that is trained on the beneficial samples to maximize its negative impact on purely uncertainty based acquisition functions. Diverging Sine samples the datapoints for each class from two diverging sinusoidal functions that are originating from the same y-intercept. This creates a challenging region on the left hand side, where a lot of datapoints need to be sampled and an easy region on the right hand side, where very few datapoints are enough. The repeating nature of a sin function encourages diversity based acquisition functions to equally sample the entire length, drastically oversampling the right hand side of the dataset. Each class has 500 datapoints. Both datasets have a budget of $B = 60$ and are tested with query sizes 1 and 5.

Results for the Honeyplot dataset reveal expected shortcomings of uncertainty sampling algorithms like margin, entropy and least confident sampling as well as BALD. In addition, BADGE is underperforming for this dataset compared to real-world data. Results for Diverging Sine also confirm expected behavior, as clustering algorithms (Coreset, TypiClust) fall behind uncertainty algorithms (Entropy-, Margin-Sampling), with the exception of BADGE.

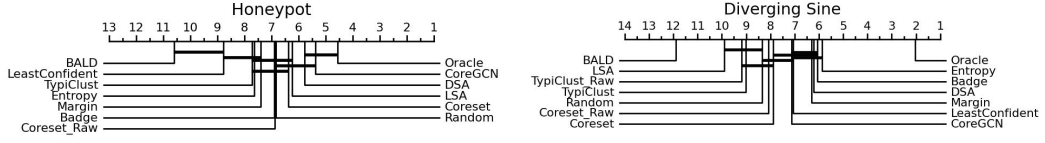
We provide a very small ablation study on the importance of the embeddings by testing a version of Coreset and TypiClust on this dataset that does not use the embeddings produced by the classification model, but rather clusters the data directly. "Coreset Raw" and "TypiClust Raw" both perform worse than their embedding-based counterpart.

8.1 Results

Our results on Honeyplot reveal principled shortcomings for the two best algorithms in BADGE and margin sampling. Both are vulnerable to adverse samples or simply measurement noise, which highlights the need for further research in this area.

Finally, the fact that BADGE is able to perform well on Diverging Sine highlights the importance of

Figure 4: Results for all acquisition functions on both synthetic datasets.



345 embeddings for the clustering algorithms, as the so-called gradient embedding from BADGE seems
 346 to be able to encode uncertainty information, guiding the selection into the left hand regions of the
 347 dataset. We also show that embeddings are generally useful for this dataset, by providing results for
 348 "Coreset Raw" and "TypiClust Raw".

349 9 Conclusion

350 We strongly advocate to test newly proposed AL algorithms not only on a wide variety of real data
 351 domains, but also to pay close attention to the Honeypot and Diverging Sine datasets to reveal princi-
 352 pled shortcomings of the algorithm in question. Both tasks can be easily carried out by implementing
 353 the new acquisition function into our code base.

354 **Acknowledgement** anonymous

355 **References**

- 356 [1] Jordan T Ash, Chicheng Zhang, Akshay Krishnamurthy, John Langford, and Alekh Agarwal.
357 Deep batch active learning by diverse, uncertain gradient lower bounds. In *International Con-*
358 *ference on Learning Representations*, 2020.
- 359 [2] Nathan Beck, Durga Sivasubramanian, Apurva Dani, Ganesh Ramakrishnan, and Rishabh
360 Iyer. Effective evaluation of deep active learning on image classification tasks. *arXiv preprint*
361 *arXiv:2106.15324*, 2021.
- 362 [3] Razvan Caramalau, Binod Bhattacharai, and Tae-Kyun Kim. Sequential graph convolutional net-
363 work for active learning. In *Proceedings of the IEEE/CVF conference on computer vision and*
364 *pattern recognition*, pages 9583–9592, 2021.
- 365 [4] Akshay L Chandra and Vineeth N Balasubramanian. Deep active learning toolkit for image
366 classification in pytorch, 2021.
- 367 [5] Ting Chen, Simon Kornblith, Mohammad Norouzi, and Geoffrey Hinton. A simple framework
368 for contrastive learning of visual representations. In *International conference on machine*
369 *learning*, pages 1597–1607. PMLR, 2020.
- 370 [6] Xilun Chen, Asish Ghoshal, Yashar Mehdad, Luke Zettlemoyer, and Sonal Gupta. Low-
371 resource domain adaptation for compositional task-oriented semantic parsing. In *Proceedings*
372 *of the 2020 Conference on Empirical Methods in Natural Language Processing (EMNLP)*.
373 Association for Computational Linguistics, 2020.
- 374 [7] Yarin Gal, Riashat Islam, and Zoubin Ghahramani. Deep bayesian active learning with image
375 data. In *International conference on machine learning*, pages 1183–1192. PMLR, 2017.
- 376 [8] Guy Hacohen, Avihu Dekel, and Daphna Weinshall. Active learning on a budget: Opposite
377 strategies suit high and low budgets. *arXiv preprint arXiv:2202.02794*, 2022.
- 378 [9] Qiang Hu, Yuejun Guo, Maxime Cordy, Xiaofei Xie, Wei Ma, Mike Papadakis, and Yves
379 Le Traon. Towards exploring the limitations of active learning: An empirical study. In *2021*
380 *36th IEEE/ACM International Conference on Automated Software Engineering (ASE)*, pages
381 917–929. IEEE, 2021.
- 382 [10] Yilin Ji, Daniel Kaestner, Oliver Wirth, and Christian Wressnegger. Randomness is the root
383 of all evil: More reliable evaluation of deep active learning. In *Proceedings of the IEEE/CVF*
384 *Winter Conference on Applications of Computer Vision*, pages 3943–3952, 2023.
- 385 [11] Jinhan Kim, Robert Feldt, and Shin Yoo. Guiding deep learning system testing using surprise
386 adequacy. In *2019 IEEE/ACM 41st International Conference on Software Engineering (ICSE)*,
387 pages 1039–1049. IEEE, 2019.
- 388 [12] Andreas Kirsch, Joost Van Amersfoort, and Yarin Gal. Batchbald: Efficient and diverse batch
389 acquisition for deep bayesian active learning. *Advances in neural information processing sys-*
390 *tems*, 32, 2019.
- 391 [13] Alex Krizhevsky, Geoffrey Hinton, et al. Learning multiple layers of features from tiny images.
392 2009.
- 393 [14] CURE Lab. Deep active learning with pytorch. [https://github.com/cure-lab/](https://github.com/cure-lab/deep-active-learning)
394 [deep-active-learning](https://github.com/cure-lab/deep-active-learning), 2022.
- 395 [15] Yu Li, Muxi Chen, Yannan Liu, Daojing He, and Qiang Xu. An empirical study on the efficacy
396 of deep active learning for image classification. *arXiv preprint arXiv:2212.03088*, 2022.

- 397 [16] David Lowell, Zachary C Lipton, and Byron C Wallace. Practical obstacles to deploying active
398 learning. *arXiv preprint arXiv:1807.04801*, 2018.
- 399 [17] Carsten Lüth, Till Bungert, Lukas Klein, and Paul Jaeger. Navigating the pitfalls of active
400 learning evaluation: A systematic framework for meaningful performance assessment. *Ad-
401 vances in Neural Information Processing Systems*, 36, 2024.
- 402 [18] Rishabh Misra. News category dataset. *arXiv preprint arXiv:2209.11429*, 2022.
- 403 [19] Prateek Munjal, Nasir Hayat, Munawar Hayat, Jamshid Sourati, and Shadab Khan. Towards ro-
404 bust and reproducible active learning using neural networks. In *Proceedings of the IEEE/CVF
405 Conference on Computer Vision and Pattern Recognition*, pages 223–232, 2022.
- 406 [20] Information Engineering Graduate Institute of Taiwan University. Libsvmtools, 2017.
- 407 [21] Jeffrey Pennington, Richard Socher, and Christopher D. Manning. Glove: Global vectors for
408 word representation. In *Empirical Methods in Natural Language Processing (EMNLP)*, pages
409 1532–1543, 2014.
- 410 [22] Lukas Rauch, Matthias Aßenmacher, Denis Huseljic, Moritz Wirth, Bernd Bischl, and Bern-
411 hard Sick. Activeglae: A benchmark for deep active learning with transformers. In *Joint
412 European Conference on Machine Learning and Knowledge Discovery in Databases*, pages
413 55–74. Springer, 2023.
- 414 [23] Ozan Sener and Silvio Savarese. Active learning for convolutional neural networks: A core-set
415 approach. *arXiv preprint arXiv:1708.00489*, 2017.
- 416 [24] Dan Wang and Yi Shang. A new active labeling method for deep learning. In *2014 Interna-
417 tional joint conference on neural networks (IJCNN)*, pages 112–119. IEEE, 2014.
- 418 [25] Han Xiao, Kashif Rasul, and Roland Vollgraf. Fashion-mnist: a novel image dataset for bench-
419 marking machine learning algorithms. *arXiv preprint arXiv:1708.07747*, 2017.
- 420 [26] Donggeun Yoo and In So Kweon. Learning loss for active learning. In *Proceedings of the
421 IEEE/CVF conference on computer vision and pattern recognition*, pages 93–102, 2019.
- 422 [27] Xueying Zhan, Huan Liu, Qing Li, and Antoni B Chan. A comparative survey: Benchmarking
423 for pool-based active learning. In *IJCAI*, pages 4679–4686, 2021.
- 424 [28] Xueying Zhan, Qingzhong Wang, Kuan-hao Huang, Haoyi Xiong, Dejing Dou, and Antoni B
425 Chan. A comparative survey of deep active learning. *arXiv preprint arXiv:2203.13450*, 2022.
- 426 [29] Yilun Zhou, Adithya Renduchintala, Xian Li, Sida Wang, Yashar Mehdad, and Asish Ghoshal.
427 Towards understanding the behaviors of optimal deep active learning algorithms. In *Interna-
428 tional Conference on Artificial Intelligence and Statistics*, pages 1486–1494. PMLR, 2021.

429 **A AL Recommendations from Ji et al.**

430 TODO

431 **B AL Pitfalls from Lueth et al.**

432 TODO

433 **C Acquisition Functions**

434 **Uncertainty Sampling** tries to find the sample that the classifier is most uncertain about by
435 computing heuristics of the class probabilities. For our benchmark, we use entropy and margin
436 (a.k.a. best-vs-second-best) sampling.

437 **BALD** [12] applies the query-by-committee strategy of model ensembles to a single model by
438 interpreting the classifier’s parameters as distributions and then sample multiple outputs from them
439 via Monte-Carlo dropout.

440 **BADGE** [1] uses gradient embeddings of unlabeled points to select samples where the classifier
441 is expected to change a lot. The higher the magnitude of the gradient the higher the expected
442 improvement in model performance.

443 **Coreset** [23] employs K-Means clustering trying to cover the whole data distribution. Selects
444 the unlabeled sample that is the furthest away from all cluster centers. Clustering is done in a
445 semantically meaningful space by encoding the data with the current classifier \hat{y} . In this work, we
446 use the greedy variant of Coreset.

447 **TypiClust** [8] relies on clustering similar to Coreset, but proposes a new measure called “Typical-
448 ity” to select unlabeled samples. It selects points that are in the densest regions of clusters that do
449 not contain labeled samples yet. Clustering is done in a semantically meaningful space by encoding
450 the data with the current classifier \hat{y} . It has to be pointed out that TypiClust was designed for
451 low-budget scenarios, but we think it is still worthwhile to test and compare this algorithm with
452 higher budgets.

453 **Core-GCN** [3] TODO

454 **DSA/LSA** [11] TODO

455 **Excluded Algorithms**

456 **Learning Loss for AL** [26] Introduces an updated training of the classification model with an
457 auxiliary loss and therefore cannot be compared fairly against classification models without this
458 boosted training regime.

459 **Reinforcement Learning Algorithms**

460

461 **D Difference of Ranks with 3 Repetitions**

462 Table 4 and Table 5 follow the exact same computation of ranks that created the main result (Table
463 3) with the only difference being a reduced number of runs per acquisition function. For each table
464 we sampled 3 runs uniformly at random from the available 50 per acquisition function.

465 We can observe significant differences between the two tables:

466 **Purple:** A multitude of rank differences of acquisition functions for specific datasets, some as high
467 as 4.7 ranks for TypiClust on the Splice dataset

468 **Olive:** Well separated acquisition functions in Tab. 5 (Margin and BADGE) are almost indistin-
469 guishable in Tab 4

470 **Red:** BALD lost 2 places in the overall ranking and Entropy gained 2

471 Even though the overall ordering of acquisition functions stayed relatively unchanged due to the
472 averaging across many datasets, each individual dataset was subject to drastic permutations. This
473 highlights the need for many repetitions in AL experiments.

Table 4: Ranks of all acquisition functions per dataset. First random draw of 3 runs from the overall pool of 50.

	Splice	DNA	USPS	Cifar10	FMnist	TopV2	News	Unencoded	Encoded
Oracle	1.0	1.0	1.0	1.0	1.0	1.0	1.0	1.0	2.1
Margin	6.0	7.3	2.0	6.7	5.3	2.3	3.3	4.7	4.4
Badge	6.0	7.3	3.0	6.7	5.0	3.3	4.0	5.0	5.3
BALD	3.3	4.7	5.3	12.0	7.0	6.3	4.3	6.1	7.9
CoreGCN	8.7	3.7	10.7	6.3	5.3	4.0	7.7	6.6	9.1
DSA	8.3	6.3	7.7	7.7	4.3	6.7	6.7	6.8	6.1
LeastConf	10.0	12.0	8.0	3.0	4.3	9.3	2.3	7.0	6.7
LSA	5.7	6.7	5.3	6.7	10.7	7.7	7.0	7.1	6.3
Entropy	11.0	3.3	7.3	4.0	6.7	8.3	9.7	7.2	7.0
Random	7.7	8.7	5.3	8.0	11.0	8.0	9.0	8.2	6.3
Coreset	4.7	10.3	10.3	7.7	6.0	9.0	11.0	8.4	7.2
TypiClust	5.7	6.7	12.0	8.3	11.3	12.0	12.0	9.7	9.7

Table 5: Ranks of all acquisition functions per dataset. Second random draw of 3 runs from the overall pool of 50.

	Splice	DNA	USPS	Cifar10	FMnist	TopV2	News	Unencoded	Encoded
Oracle	1.0	1.0	1.0	1.0	1.0	1.0	1.0	1.0	2.4
Margin	6.0	3.3	2.0	5.7	2.0	2.0	4.3	3.6	3.8
Badge	6.0	9.0	3.0	3.0	5.7	3.7	3.3	4.8	4.9
CoreGCN	4.3	6.3	10.3	7.3	5.3	5.7	5.3	6.4	8.1
DSA	8.7	7.3	7.3	6.0	4.3	5.3	6.0	6.4	6.5
BALD	4.7	4.0	4.7	12.0	7.3	6.7	6.7	6.6	7.5
Entropy	6.7	4.7	7.7	5.3	5.0	7.3	9.3	6.6	6.8
LeastConf	7.7	10.0	8.3	3.3	6.0	8.7	3.0	6.7	7.3
LSA	7.7	5.3	6.0	9.0	11.0	9.0	7.3	7.9	7.5
Random	9.3	8.0	5.0	8.7	11.7	8.3	8.7	8.5	7.6
Coreset	6.0	10.7	10.7	8.0	8.3	8.3	11.0	9.0	6.3
TypiClust	10.0	8.3	12.0	8.7	10.3	12.0	12.0	10.5	9.4

474 E AUCs by Query Size

Table 6: AUC values for each dataset that supports query size 1.

	Splice	SpliceEncoded	DNA	DNAEncoded	USPS	USPSEncoded	Cifar10Encoded	FashionMnistEnc	TopV2	DivergingSin	ThreeClust
Oracle	0.803+-0.012	0.678+-0.021	0.825+-0.009	0.721+-0.013	0.866+-0.004	0.436+-0.057	0.749+-0.009	0.755+-0.005	0.884+-0.006	0.957+-0.009	0.783+-0.03
Margin	0.769+-0.021	0.678+-0.032	0.806+-0.013	0.642+-0.047	0.858+-0.006	0.426+-0.038	0.653+-0.013	0.68+-0.012	0.861+-0.009	0.941+-0.018	0.704+-0.074
Badge	0.767+-0.02	0.661+-0.026	0.78+-0.014	0.642+-0.046	0.83+-0.008	0.371+-0.035	0.656+-0.013	0.68+-0.009	0.826+-0.024	0.941+-0.017	0.69+-0.083
LeastConfident	0.779+-0.019	0.68+-0.032	0.809+-0.01	0.629+-0.05	0.846+-0.009	0.421+-0.039	0.668+-0.014	0.685+-0.009	0.843+-0.013	0.94+-0.016	0.692+-0.094
DSA	0.766+-0.021	0.691+-0.022	0.803+-0.01	0.646+-0.032	0.829+-0.01	0.431+-0.05	0.663+-0.014	0.679+-0.01	0.844+-0.017	0.941+-0.014	0.731+-0.032
BALD	0.78+-0.014	0.649+-0.04	0.784+-0.01	0.632+-0.042	0.819+-0.01	0.242+-0.046	0.666+-0.014	0.644+-0.018	0.815+-0.024	0.928+-0.014	0.698+-0.043
CoreGCN	0.765+-0.021	0.686+-0.023	0.804+-0.012	0.646+-0.03	0.753+-0.016	0.39+-0.044	0.623+-0.018	0.647+-0.012	0.85+-0.01	0.938+-0.014	0.731+-0.028
Entropy	0.768+-0.022	0.678+-0.035	0.812+-0.013	0.635+-0.045	0.83+-0.011	0.399+-0.035	0.663+-0.013	0.681+-0.011	0.815+-0.021	0.942+-0.017	0.696+-0.083
LSA	0.772+-0.016	0.68+-0.026	0.787+-0.012	0.618+-0.036	0.821+-0.009	0.422+-0.037	0.613+-0.014	0.642+-0.012	0.816+-0.013	0.932+-0.016	0.727+-0.033
Random	0.76+-0.016	0.674+-0.027	0.774+-0.013	0.63+-0.035	0.823+-0.009	0.404+-0.036	0.613+-0.014	0.639+-0.013	0.815+-0.012	0.933+-0.017	0.721+-0.036
Coreset	0.772+-0.016	0.69+-0.017	0.79+-0.012	0.638+-0.041	0.767+-0.016	0.404+-0.046	0.659+-0.011	0.684+-0.009	0.826+-0.022	0.937+-0.014	0.734+-0.031
TypiClust	0.762+-0.016	0.685+-0.025	0.778+-0.01	0.663+-0.028	0.828+-0.007	0.396+-0.046	0.653+-0.013	0.649+-0.007	0.831+-0.011	0.934+-0.018	0.727+-0.033

Table 7: AUC values for each dataset that supports query size 5.

	Splice	SpliceEncoded	DNA	DNAEncoded	USPS	USPSEncoded	Cifar10Encoded	FashionMnistEncoded	TopV2	DivergingSin	ThreeClust
Oracle	0.803+-0.012	0.678+-0.021	0.825+-0.009	0.721+-0.013	0.866+-0.004	0.436+-0.057	0.749+-0.009	0.755+-0.005	0.884+-0.006	0.957+-0.009	0.783+-0.03
Margin	0.765+-0.021	0.662+-0.032	0.794+-0.011	0.611+-0.05	0.855+-0.006	0.508+-0.02	0.656+-0.014	0.678+-0.009	0.848+-0.013	0.923+-0.019	0.697+-0.055
Badge	0.768+-0.014	0.646+-0.035	0.785+-0.011	0.624+-0.036	0.846+-0.007	0.48+-0.021	0.647+-0.012	0.674+-0.009	0.847+-0.01	0.924+-0.019	0.72+-0.036
LeastConfident	0.763+-0.023	0.643+-0.034	0.798+-0.013	0.585+-0.065	0.831+-0.014	0.478+-0.028	0.67+-0.01	0.681+-0.009	0.819+-0.023	0.921+-0.019	0.675+-0.072
DSA	0.765+-0.023	0.653+-0.029	0.793+-0.009	0.613+-0.034	0.822+-0.01	0.489+-0.024	0.661+-0.013	0.662+-0.012	0.833+-0.02	0.924+-0.018	0.718+-0.034
BALD	0.775+-0.018	0.641+-0.034	0.801+-0.013	0.592+-0.054	0.84+-0.008	0.332+-0.054	0.681+-0.011	0.681+-0.011	0.824+-0.023	0.893+-0.035	0.673+-0.041
CoreGCN	0.759+-0.018	0.662+-0.027	0.79+-0.011	0.62+-0.03	0.755+-0.011	0.45+-0.03	0.604+-0.016	0.609+-0.013	0.837+-0.014	0.922+-0.018	0.723+-0.034
Entropy	0.765+-0.022	0.66+-0.03	0.798+-0.011	0.611+-0.054	0.823+-0.013	0.464+-0.024	0.663+-0.013	0.672+-0.011	0.801+-0.025	0.924+-0.02	0.689+-0.066
LSA	0.769+-0.016	0.654+-0.032	0.781+-0.013	0.61+-0.041	0.82+-0.009	0.484+-0.022	0.617+-0.012	0.641+-0.011	0.816+-0.012	0.915+-0.018	0.718+-0.038
Random	0.758+-0.015	0.655+-0.026	0.771+-0.013	0.623+-0.031	0.82+-0.009	0.476+-0.024	0.616+-0.016	0.637+-0.012	0.812+-0.014	0.921+-0.018	0.713+-0.034
Coreset	0.765+-0.017	0.663+-0.023	0.784+-0.014	0.603+-0.034	0.765+-0.015	0.449+-0.022	0.657+-0.009	0.674+-0.009	0.817+-0.017	0.92+-0.017	0.713+-0.035
TypiClust	0.759+-0.014	0.641+-0.028	0.775+-0.01	0.603+-0.04	0.757+-0.02	0.465+-0.027	0.596+-0.014	0.567+-0.012	0.727+-0.026	0.916+-0.02	0.693+-0.045

Table 8: AUC values for each dataset that supports query size 20.

	Splice	SpliceEncoded	DNA	USPS	USPSEncoded	Cifar10Encoded	FashionMnistEnc	TopV2	News
Oracle	0.803+-0.012	0.678+-0.021	0.825+-0.009	0.866+-0.004	0.436+-0.057	0.749+-0.009	0.755+-0.005	0.884+-0.006	0.49+-0.003
Margin	0.759+-0.027	0.618+-0.04	0.779+-0.013	0.847+-0.008	0.439+-0.027	0.656+-0.01	0.67+-0.011	0.823+-0.014	0.464+-0.007
Badge	0.767+-0.013	0.619+-0.033	0.776+-0.013	0.845+-0.006	0.44+-0.019	0.647+-0.013	0.665+-0.007	0.827+-0.016	0.463+-0.007
LeastConfident	0.751+-0.02	0.597+-0.05	0.748+-0.025	0.798+-0.027	0.391+-0.024	0.665+-0.013	0.669+-0.011	0.775+-0.035	0.467+-0.008
DSA	0.759+-0.02	0.599+-0.034	0.769+-0.013	0.809+-0.012	0.421+-0.023	0.647+-0.014	0.63+-0.013	0.793+-0.026	0.459+-0.01
BALD	0.768+-0.022	0.57+-0.037	0.784+-0.015	0.822+-0.009	0.298+-0.039	0.675+-0.008	0.673+-0.01	0.789+-0.024	0.468+-0.009
CoreGCN	0.759+-0.018	0.612+-0.039	0.774+-0.012	0.754+-0.016	0.397+-0.026	0.587+-0.015	0.583+-0.015	0.807+-0.018	0.453+-0.006
Entropy	0.759+-0.027	0.618+-0.038	0.773+-0.015	0.803+-0.019	0.372+-0.022	0.656+-0.011	0.65+-0.012	0.773+-0.031	0.451+-0.007
LSA	0.761+-0.014	0.611+-0.039	0.768+-0.015	0.816+-0.009	0.411+-0.022	0.621+-0.01	0.635+-0.011	0.796+-0.016	0.452+-0.007
Random	0.755+-0.014	0.612+-0.039	0.763+-0.012	0.818+-0.009	0.439+-0.019	0.622+-0.013	0.633+-0.012	0.795+-0.016	0.45+-0.006
Coreset	0.759+-0.016	0.601+-0.034	0.764+-0.015	0.757+-0.015	0.39+-0.029	0.647+-0.009	0.651+-0.011	0.784+-0.026	0.435+-0.012
TypiClust	0.751+-0.012	0.551+-0.036	0.76+-0.016	0.643+-0.026	0.411+-0.024	0.488+-0.02	0.449+-0.017	0.652+-0.035	0.406+-0.011

Table 9: AUC values for each dataset that supports query size 50.

	Splice	DNA	USPS	USPSEncoded	Cifar10Encoded	FashionMnistEnc	TopV2	News
Oracle	0.803+-0.012	0.825+-0.009	0.866+-0.004	0.436+-0.057	0.749+-0.009	0.755+-0.005	0.884+-0.006	0.49+-0.003
Margin	0.747+-0.023	0.751+-0.019	0.828+-0.009	0.363+-0.031	0.64+-0.013	0.653+-0.01	0.774+-0.029	0.46+-0.006
Badge	0.758+-0.017	0.754+-0.018	0.831+-0.008	0.376+-0.028	0.632+-0.013	0.649+-0.011	0.781+-0.026	0.462+-0.007
LeastConfident	0.731+-0.025	0.688+-0.041	0.761+-0.037	0.291+-0.03	0.644+-0.013	0.65+-0.011	0.73+-0.049	0.462+-0.009
DSA	0.748+-0.021	0.738+-0.018	0.783+-0.016	0.346+-0.027	0.624+-0.014	0.588+-0.016	0.748+-0.041	0.45+-0.011
BALD	0.76+-0.017	0.756+-0.018	0.796+-0.016	0.241+-0.026	0.65+-0.009	0.645+-0.01	0.746+-0.038	0.455+-0.007
CoreGCN	0.755+-0.016	0.745+-0.018	0.752+-0.019	0.328+-0.027	0.581+-0.015	0.568+-0.018	0.771+-0.025	0.453+-0.007
Entropy	0.747+-0.024	0.748+-0.018	0.778+-0.024	0.275+-0.026	0.633+-0.011	0.625+-0.012	0.734+-0.036	0.442+-0.007
LSA	0.754+-0.013	0.749+-0.019	0.807+-0.01	0.341+-0.029	0.613+-0.012	0.625+-0.01	0.763+-0.025	0.45+-0.006
Random	0.746+-0.012	0.745+-0.015	0.806+-0.008	0.379+-0.028	0.615+-0.014	0.621+-0.01	0.759+-0.026	0.448+-0.006
Coreset	0.751+-0.016	0.733+-0.019	0.74+-0.017	0.325+-0.034	0.624+-0.012	0.608+-0.013	0.731+-0.045	0.432+-0.012
TypiClust	0.749+-0.016	0.736+-0.016	0.586+-0.038	0.348+-0.027	0.451+-0.024	0.375+-0.022	0.614+-0.046	0.397+-0.012

Table 10: AUC values for each dataset that supports query size 100.

	Splice	DNA	USPS	USPSEncoded	Cifar10Encoded	FashionMnistEnc	News
Oracle	0.803+-0.012	0.825+-0.009	0.866+-0.004	0.436+-0.057	0.749+-0.009	0.755+-0.005	0.49+-0.003
Margin	0.733+-0.024	0.711+-0.027	0.799+-0.013	0.473+-0.026	0.629+-0.012	0.628+-0.009	0.455+-0.006
Badge	0.743+-0.014	0.714+-0.032	0.804+-0.013	0.472+-0.029	0.623+-0.01	0.621+-0.01	0.456+-0.006
LeastConfident	0.715+-0.033	0.639+-0.05	0.708+-0.034	0.23+-0.034	0.631+-0.013	0.62+-0.012	0.457+-0.008
DSA	0.729+-0.021	0.697+-0.031	0.753+-0.021	0.427+-0.028	0.609+-0.013	0.546+-0.017	0.442+-0.01
BALD	0.744+-0.015	0.718+-0.024	0.765+-0.021	0.285+-0.046	0.632+-0.009	0.609+-0.01	0.444+-0.007
CoreGCN	0.742+-0.015	0.713+-0.025	0.744+-0.019	0.433+-0.032	0.583+-0.013	0.554+-0.015	0.448+-0.007
Entropy	0.733+-0.023	0.713+-0.031	0.743+-0.026	0.395+-0.037	0.618+-0.012	0.59+-0.012	0.432+-0.007
LSA	0.738+-0.017	0.716+-0.027	0.789+-0.011	0.439+-0.03	0.609+-0.013	0.608+-0.01	0.447+-0.006
Random	0.733+-0.013	0.713+-0.023	0.789+-0.012	0.468+-0.024	0.611+-0.01	0.606+-0.01	0.446+-0.005
Coreset	0.735+-0.019	0.698+-0.026	0.721+-0.021	0.396+-0.024	0.608+-0.012	0.562+-0.016	0.426+-0.012
TypiClust	0.733+-0.016	0.704+-0.025	0.592+-0.042	0.427+-0.027	0.501+-0.02	0.338+-0.02	0.383+-0.012

Table 11: AUC values for each dataset that supports query size 500.

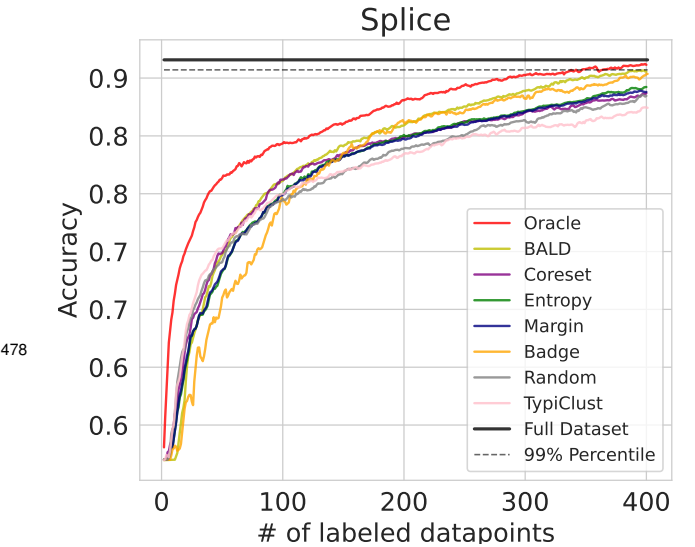
	Cifar10	FashionMnist
Oracle	0.689+-0.001	0.905+-0.001
Margin	0.556+-0.008	0.882+-0.004
Badge	0.56+-0.008	0.883+-0.005
LeastConfident	0.591+-0.01	0.884+-0.005
DSA	0.56+-0.009	0.882+-0.004
BALD	0.478+-0.014	0.878+-0.003
CoreGCN	0.553+-0.01	0.88+-0.007
Entropy	0.553+-0.009	0.882+-0.006
LSA	0.558+-0.01	0.866+-0.005
Random	0.557+-0.01	0.863+-0.005
Coreset	0.553+-0.007	0.878+-0.006
TypiClust	0.557+-0.009	0.864+-0.004

Table 12: AUC values for each dataset that supports query size 1000.

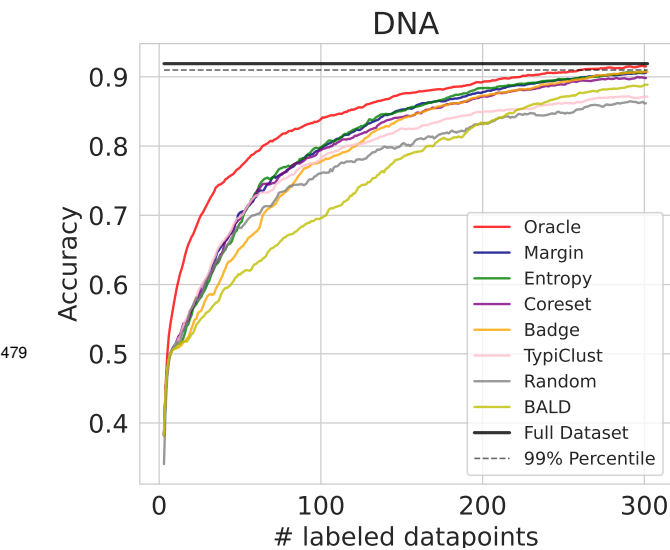
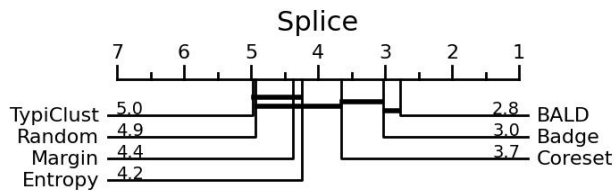
	Cifar10	FashionMnist
Oracle	0.689+-0.001	0.905+-0.001
Margin	0.56+-0.011	0.872+-0.007
Badge	0.562+-0.013	0.871+-0.007
LeastConfident	0.561+-0.012	0.873+-0.006
DSA	0.56+-0.011	0.87+-0.008
BALD	0.535+-0.011	0.866+-0.003
CoreGCN	0.557+-0.011	0.867+-0.012
Entropy	0.557+-0.014	0.871+-0.009
LSA	0.551+-0.012	0.854+-0.009
Random	0.55+-0.01	0.855+-0.006
Coreset	0.562+-0.012	0.869+-0.004
TypiClust	0.552+-0.011	0.854+-0.009

476 **F Critical Difference Diagrams**

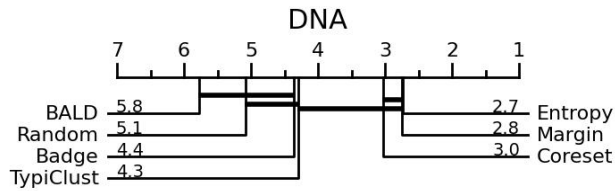
477 **G Individual Results**

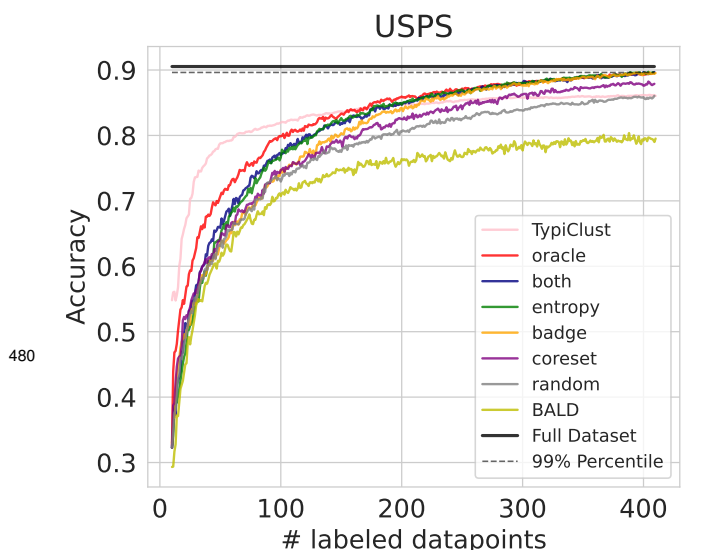


	Splice
Oracle	0.811 ± 0.010
BALD	0.785 ± 0.013
Coreset	0.778 ± 0.014
Entropy	0.774 ± 0.016
Margin	0.773 ± 0.016
Badge	0.770 ± 0.016
Random	0.768 ± 0.014
TypiClust	0.766 ± 0.014

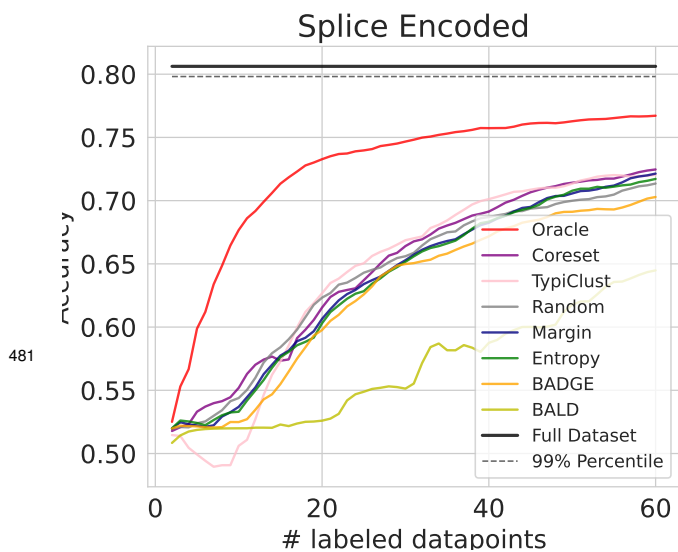
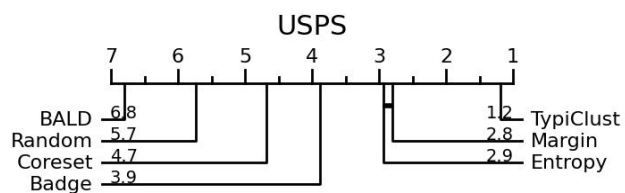


	DNA
Oracle	0.842 ± 0.021
Margin	0.807 ± 0.035
Entropy	0.805 ± 0.038
Coreset	0.796 ± 0.028
Badge	0.789 ± 0.056
TypiClust	0.788 ± 0.036
Random	0.768 ± 0.024
BALD	0.749 ± 0.044

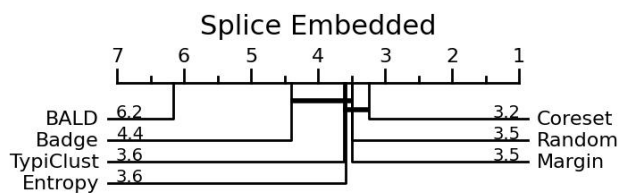


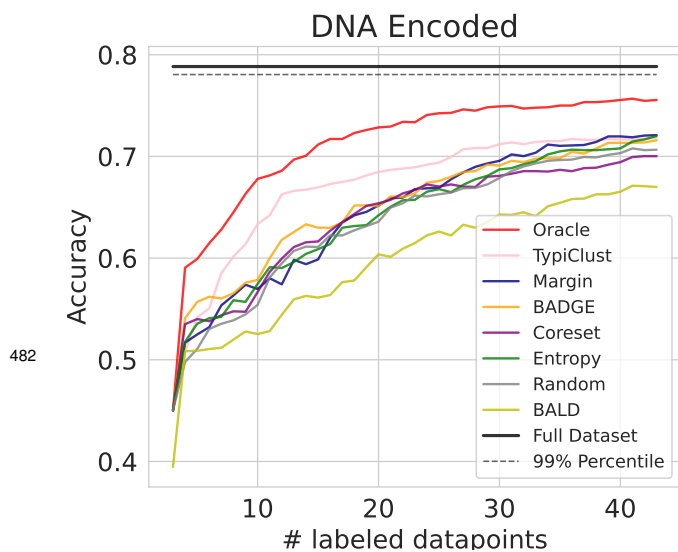


	USPS
TypiClust	0.830 ± 0.007
Oracle	0.823 ± 0.011
Margin	0.809 ± 0.013
Entropy	0.807 ± 0.013
Badge	0.795 ± 0.018
Coreset	0.788 ± 0.017
Random	0.774 ± 0.012
BALD	0.725 ± 0.050

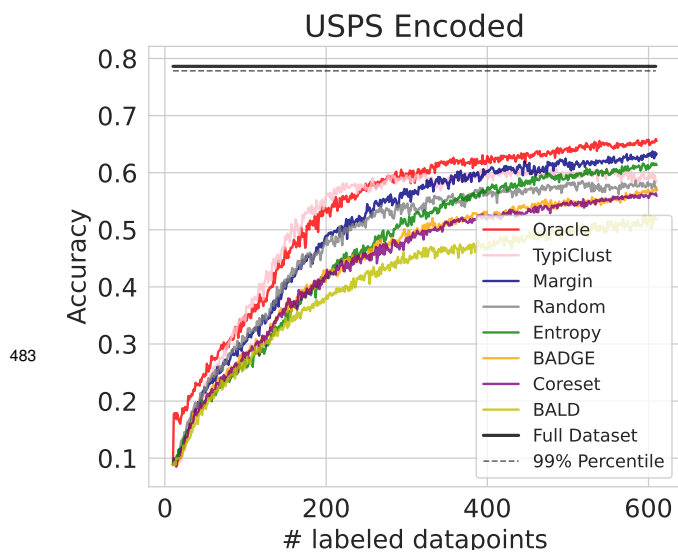
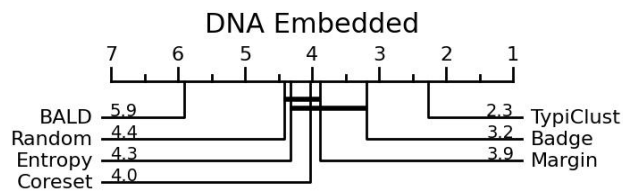


	SpliceEncoded
Oracle	0.728 ± 0.022
Coreset	0.648 ± 0.027
TypiClust	0.645 ± 0.042
Random	0.643 ± 0.036
Entropy	0.636 ± 0.033
Margin	0.636 ± 0.033
Badge	0.627 ± 0.040
BALD	0.565 ± 0.049

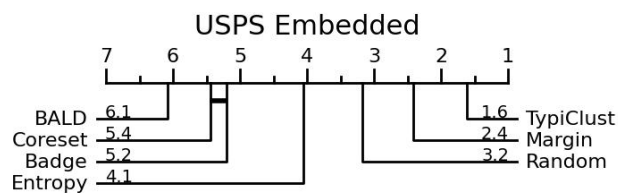


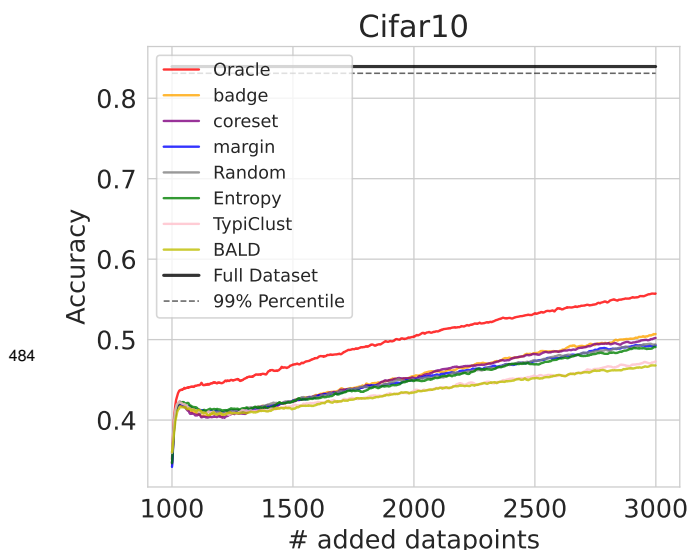


	DNAEncoded
Oracle	0.709 ± 0.023
TypiClust	0.672 ± 0.029
Margin	0.648 ± 0.047
Badge	0.647 ± 0.037
Coreset	0.640 ± 0.041
Entropy	0.629 ± 0.062
Random	0.626 ± 0.035
BALD	0.594 ± 0.039

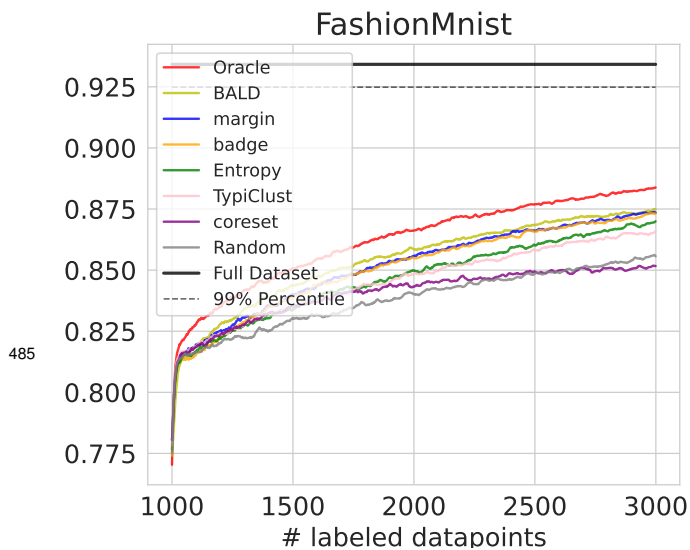
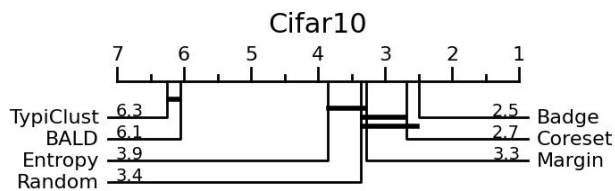


	USPSEncoded
Oracle	0.522 ± 0.021
TypiClust	0.507 ± 0.025
Margin	0.496 ± 0.030
Random	0.468 ± 0.025
Entropy	0.459 ± 0.021
Badge	0.440 ± 0.026
Coreset	0.435 ± 0.027
BALD	0.402 ± 0.052

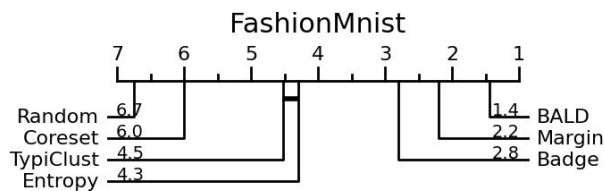


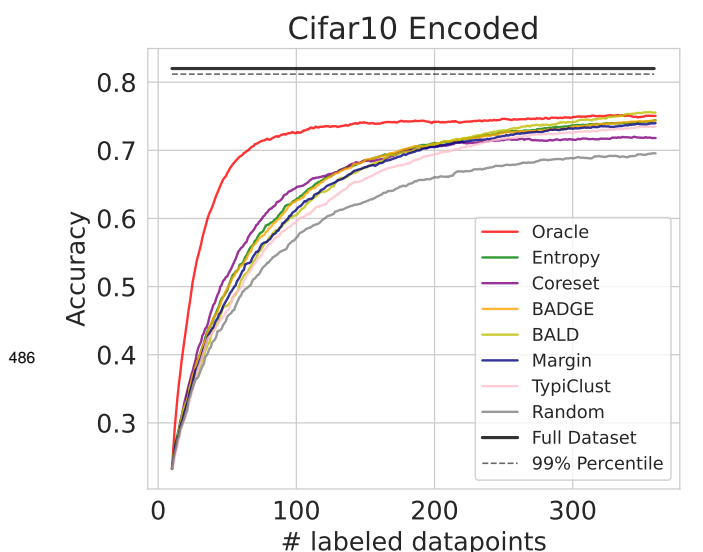


	Cifar10
Oracle	0.500 ± 0.010
Badge	0.453 ± 0.012
Coreset	0.453 ± 0.009
Margin	0.451 ± 0.010
Random	0.450 ± 0.012
Entropy	0.449 ± 0.010
TypiClust	0.436 ± 0.010
BALD	0.436 ± 0.010

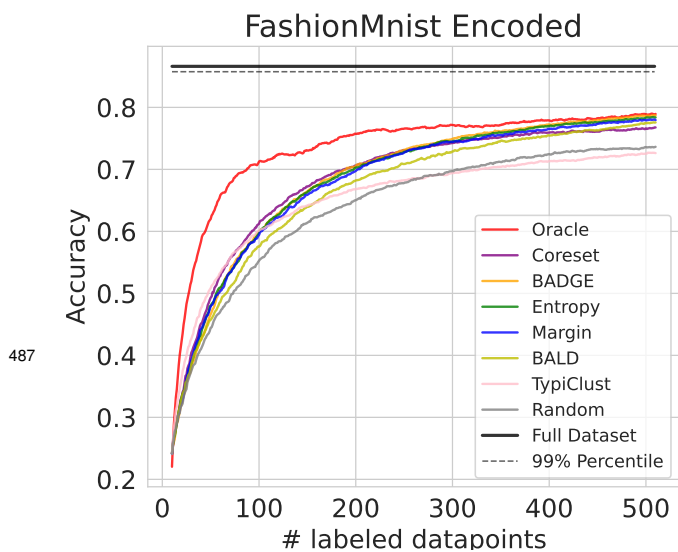
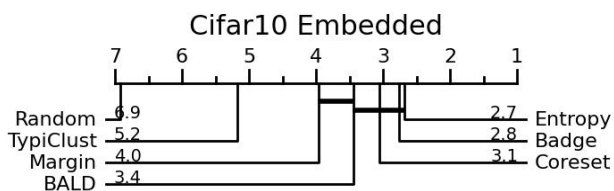


	FashionMnist
Oracle	0.862 ± 0.003
BALD	0.854 ± 0.003
Margin	0.851 ± 0.003
Badge	0.851 ± 0.003
Entropy	0.847 ± 0.004
TypiClust	0.846 ± 0.004
Coreset	0.840 ± 0.004
Random	0.837 ± 0.004

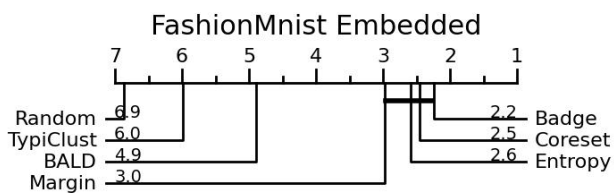


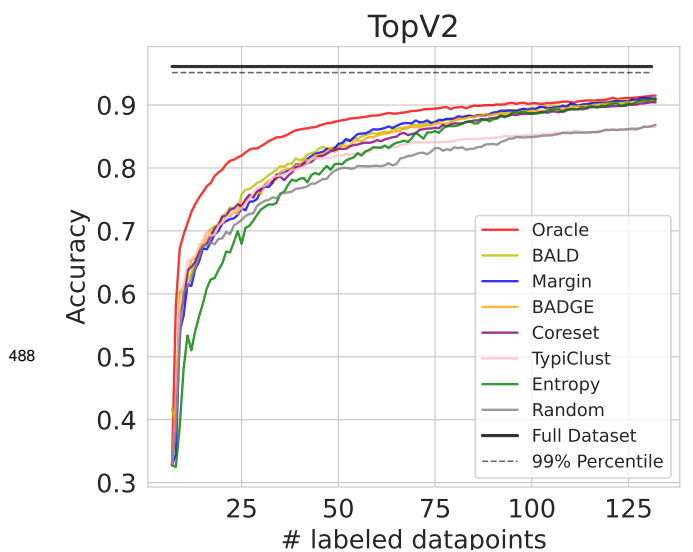


	Cifar10Encoded
Oracle	0.714 ± 0.007
Entropy	0.654 ± 0.013
Coreset	0.653 ± 0.012
Badge	0.653 ± 0.012
BALD	0.650 ± 0.016
Margin	0.647 ± 0.012
TypiClust	0.636 ± 0.009
Random	0.607 ± 0.013

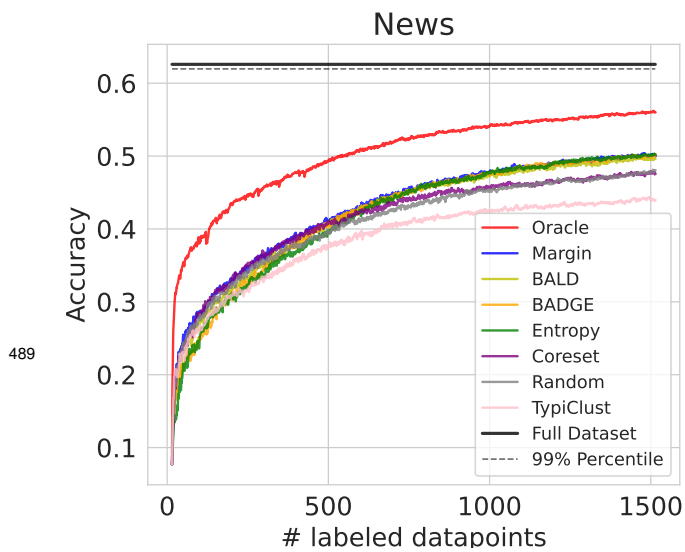
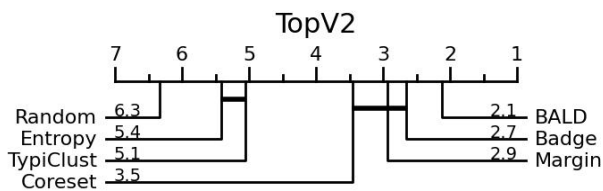


	FashionMnistEncoded
Oracle	0.732 ± 0.006
Coreset	0.686 ± 0.008
Badge	0.685 ± 0.008
Entropy	0.684 ± 0.009
Margin	0.682 ± 0.011
BALD	0.668 ± 0.009
TypiClust	0.652 ± 0.009
Random	0.640 ± 0.011

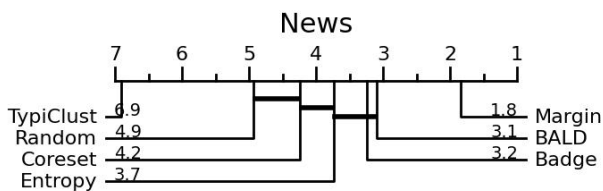


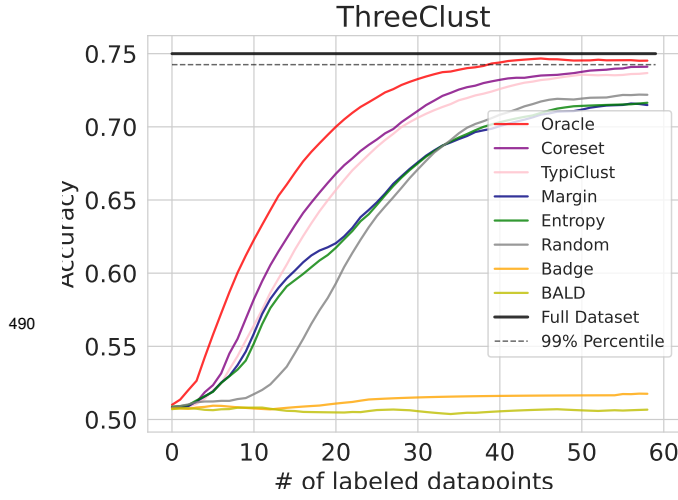


	TopV2
Oracle	0.862 ± 0.006
BALD	0.831 ± 0.013
Badge	0.826 ± 0.015
Coreset	0.823 ± 0.016
Margin	0.822 ± 0.015
TypiClust	0.805 ± 0.015
Entropy	0.801 ± 0.025
Random	0.787 ± 0.015

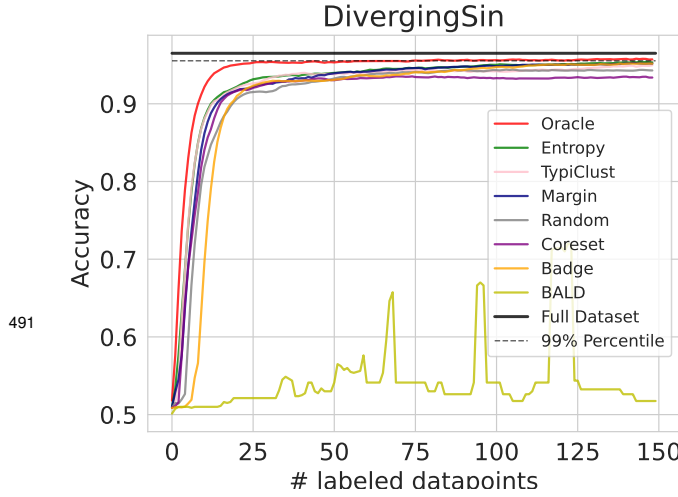
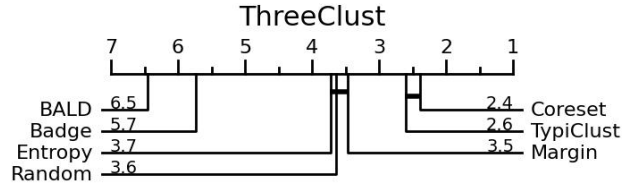


	News
Oracle	0.502 ± 0.005
Margin	0.427 ± 0.007
BALD	0.421 ± 0.008
Badge	0.420 ± 0.011
Entropy	0.416 ± 0.010
Coreset	0.415 ± 0.011
Random	0.409 ± 0.008
TypiClust	0.385 ± 0.010

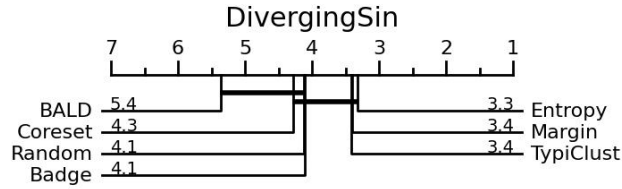




	ThreeClust
Oracle	0.722 ± 0.097
Coreset	0.698 ± 0.058
TypiClust	0.697 ± 0.055
Entropy	0.682 ± 0.098
Random	0.672 ± 0.067
Margin	0.669 ± 0.095
Badge	0.524 ± 0.086
BALD	0.507 ± 0.050



	DivergingSin
Oracle	0.948 ± 0.198
Entropy	0.936 ± 0.202
TypiClust	0.930 ± 0.196
Margin	0.929 ± 0.201
Random	0.919 ± 0.191
Badge	0.914 ± 0.202
Coreset	0.914 ± 0.197
BALD	0.661 ± 0.167



492 H Seeding Strategy

493 We aim to provide an experimental setup that is fully reproducible independent of the dataset, classi-
 494 fication model, or AL algorithm used. For a fair comparison of two AL algorithms, both algorithms
 495 need to receive equal starting conditions in terms of train/validation split, initialization of classifier,

and even the state of minor systems like the optimizer or mini-batch sampler. Even though different implementations might have their own solution to some of these problems, only [10] has described and implemented a fully reproducible pipeline for AL evaluation. The term reproducibility in this work is used as a synonym not only for the reproducibility of an experiment (a final result given a seed), but also the reproducibility of all subsystems independent of each other. The seed for one subsystem should always reproduce the behavior of this subsystem independent of all other subsystems and their seeds. The main obstacle for ensuring reproducibility is the seeding utility in PyTorch, Tensorflow, and other frameworks, whose default choice is a single global seed. Since many subsystems draw random numbers from this seed, all of them influence each other to a point where a single additional draw can completely change the model initialization, data split or the order of training batches. Even though some workarounds exist, e.g. re-setting the seed multiple times, this problem is not limited to the initialization phase, but also extends to the AL iterations and the systems within. We propose an implementation that creates separate Random Number Generators (RNGs) for each of these systems to ensure equal testing conditions even when the AL algorithm, dataset, or classifier changes. We hypothesize that the insufficient setup with global seeds contributes to the ongoing problem of inconsistent results of AL algorithms in different papers.

In summary, we introduce three different seeds: s_Ω for the AL algorithm, $s_\mathcal{D}$ for dataset splitting and mini-batch sampling, and s_θ for model initialization and sampling of dropout masks. Unless stated otherwise, we will keep s_Ω fixed, while $s_\mathcal{D}$ and s_θ are incremented by 1 between restarts to introduce stochasticity into our framework. Some algorithms require a subsample to be drawn from \mathcal{U} in order to reduce the computational cost in each iteration, while others need access to the full unlabeled pool (e.g. for effective clustering). If a subsample is required, it will be drawn from s_Ω and therefore will not influence other systems in the experiments. For each algorithm, we decided if subsampling is required based on our available hardware, but decided against setting a fixed time limit per experiment, since this would introduce unnecessary complexity into the benchmark. An overview of selected hyperparameters per AL algorithm can be found in Appendix J.

Note: Even though we decoupled the subsystems via the described seeds, the subsystems can still influence each other in a practical sense. For example, keeping $s_\mathcal{D}$ fixed does not mean that always the same sequence of samples from \mathcal{U} (if subsamples are drawn) are shown to all acquisition functions. This is practically impossible, as different acquisition functions pick different $x^{(i)}$. However, the hypothetical **tree** of all possible sequences of samples from \mathcal{U} remains the same, granting every acquisition function equal possibilities.

I Oracle Curve Forecasting

TODO

J Hyperparameters per AL Algorithm

Table 13: Selected hyperparameters for all tested acquisition functions. Last column indicates the source of our implementation.

Algorithm	Sample Size	Other	Source
BADGE	100	Dropout Trials: 5	Based on [1, 14]
BALD	100		Based on [4]
Coreset	8000		Own
TypiClust	10000	Min Cluster Size: 5 Max # Clusters: 500	Based on [8]
Margin	8000		Own
Entropy	8000		Own

531 K Hyperparameters and Preprocessing per Dataset

532 For all our datasets we use the pre-defined train/test splits, if given. In the remaining cases, we
 533 define test sets upfront and store them into separate files to keep them fixed across all experiments.
 534 The validation set is split in the experiment run itself and depends on the dataset-seed.
 535 **Tabular:** We use **Splice**, **DNA** and **USPS** from LibSVMTools [20]. All three datasets are normal-
 536 ized between [0, 1].
 537 **Image:** We use **FashionMNIST** [25] and **Cifar10** [13], since both are widely used in AL literature.
 538 Both datasets are normalized according to their standard protocols.
 539 **Text:** We use **News Category** [18] and **TopV2** [6]. For News Category we use the 15 most com-
 540 mon categories as indicated by its Kaggle site. We additionally drop sentences above 80 words to
 541 reduce the padding needed (retaining 99,86% of the data). For TopV2, we are only using the "alarm"
 542 domain. Both datasets are encoded with pre-trained GloVe (Common Crawl 840B Tokens) embed-
 543 dings [21]. Since neither dataset provided a fixed test set, we randomly split 7000 datapoints into a
 544 test set.

Dataset	Seed Set	Budget	Val Split
Splice	1	400	0.2
SpliceEnc.	1	60	0.2
DNA	1	300	0.2
DNAEnc	1	40	0.2
USPS	1	400	0.2
USPSEnc	1	600	0.2
FashionMnist	100	2000	0.04
FashionMnistEnc	1	500	0.04
Cifar10	100	2000	0.04
Cifar10Enc	1	350	0.04
TopV2	1	125	0.25
News	1	1500	0.03

Table 14: Size of the seed set is given by number of labeled sample per class.

Dataset	Classifier	Optimizer	LR	Weight Decay	Dropout	Batch Size
Splice	[24, 12]	NAdam	1.2e-3	5.9e-5	0	43
SpliceEnc.	linear	NAdam	6.2e-4	5.9e-6	0	64
DNA	[24, 12]	NAdam	3.9e-2	3.6e-5	0	64
DNAEnc	linear	NAdam	1.6e-3	4e-4	0	64
USPS	[24, 12]	Adam	8.1e-3	1.5e-6	0	43
USPSEnc	linear	NAdam	7.8e-3	1.9e-6	0	64
FashionMnist	ResNet18	NAdam	1e-3	0	0	64
FashionMnistEnc	linear	Adam	1.6e-3	1e-5	5e-2	64
Cifar10	ResNet18	NAdam	1e-3	0	0	64
Cifar10Enc	linear	NAdam	1.7e-3	2.3e-5	0	64
TopV2	BiLSTM	NAdam	1.5e-3	1.7e-7	5e-2	64
News	BiLSTM	NAdam	1.5e-3	1.7e-7	5e-2	64

Table 15: Classifier architectures and optimized hyperparameters per dataset. Numbers in brackets signify a MLP with corresponding hidden layers.

Algorithm 1 Active Learning Loop**Require:** $\mathcal{L}, \mathcal{U}, \mathcal{D}_{\text{test}}, \text{Train}, \text{Seed}, \hat{y}$ **Require:** Ω

▷ Acquisition Function

▷ Create the initial labeled set

```

1:  $\mathcal{L}^{(1)} \leftarrow \text{Seed}(\mathcal{U})$ 
2:  $\mathcal{U}^{(1)} \leftarrow \mathcal{U}$ 
3: for  $i := 1 \dots B$  do
4:    $\text{acc}^{(i)} \leftarrow \text{Train}(\mathcal{L}^{(i)})$ 
5:    $a^{(i)} \leftarrow \Omega(\mathcal{U}^{(i)})$ 
6:    $\mathcal{L}^{(i+1)} \leftarrow \mathcal{L}^{(i)} \cup \{(\mathcal{U}_a^{(i)}, A(\mathcal{U}_a^{(i)}))\}$ 
7:    $\mathcal{U}^{(i+1)} \leftarrow \mathcal{U}^{(i)} \setminus \{\mathcal{U}_a^{(i)}\}$ 
8: return  $\frac{1}{B} \sum_{i=1}^B \text{acc}^{(i)}$ 

```

Algorithm 2 Retrain**Require:** $\mathcal{L}, \mathcal{D}_{\text{val}}, \mathcal{D}_{\text{test}}$ **Require:** \hat{y}, e_{max}

```

1:  $\text{loss}^* \leftarrow \infty$ 
2: for  $i := 1 \dots e_{\text{max}}$  do
3:    $\hat{y}_{i+1} \leftarrow \hat{y}_i - \eta \nabla_{\hat{y}} \ell(\mathcal{L}, \hat{y})$ 
4:    $\text{loss}_i \leftarrow \ell(\mathcal{D}_{\text{val}}, \hat{y})$ 
5:   if  $\text{loss}_i < \text{loss}^*$  then
6:      $\text{loss}^* \leftarrow \text{loss}_i$ 
7:   else
8:     Break
9: return  $\text{Acc}(\mathcal{D}_{\text{test}}, \hat{y})$ 

```

Algorithm 3 Acquire Oracle Ω **Require:** $\mathcal{U}, \mathcal{L}, A, \mathcal{D}_{\text{test}}, \tau, \hat{y}_{\theta}$ **Require:** $\text{Train}, \text{Margin}, \text{Acc}$

```

1:  $\text{acc}^0 \leftarrow \text{acc}^* \leftarrow \text{Acc}(\mathcal{D}_{\text{test}}, \hat{y}_{\theta})$ 
2: for  $k := 1 \dots \tau$  do
3:    $u_k = \text{unif}(\mathcal{U})$ 
4:    $\mathcal{L}' \leftarrow \mathcal{L}^{(i)} \cup \{(u_k, A(u_k))\}$ 
5:    $\hat{y}'_{\theta} \leftarrow \text{Train}(\mathcal{L}', \hat{y}_{\theta})$ 
6:    $\text{acc}' \leftarrow \text{Acc}(\mathcal{D}_{\text{test}}, \hat{y}'_{\theta})$ 
7:   if  $\text{acc}' > \text{acc}^*$  then
8:      $\text{acc}^* \leftarrow \text{acc}'$ 
9:      $u^* \leftarrow u_k$ 
10: if  $\text{acc}^0 = \text{acc}^*$  then
11:    $u^* \leftarrow \text{Margin}(\mathcal{U}, \hat{y}_{\theta})$ 
return  $u^*$ 

```

546 Alg. 3 replaces the acquisition function Ω in the AL loop (Alg. L line 5).